SDSS'Rio 2010 STABILITY AND DUCTILITY OF STEEL STRUCTURES
E. Batista, P. Vellasco, L. de Lima (Eds.)
Rio de Janeiro, Brazil, September 8 - 10, 2010

EFFECTS OF DISTORTION ON THE SHEAR STIFFNESS OF RACK STRUCTURES

Sambasiva R. Sajja*, Robert G. Beale and Michael H.R. Godley***

* School of the Built Environment, Oxford Brookes University, Oxford, UK
** School of Technology, Oxford Brookes University, Oxford, UK
e-mails: srsajja@gmail.com, rgbeale@brookes.ac.uk, mgodley@brookes.ac.uk

Keywords: Stability; Distortion, Built-up columns; Shear stiffness; Pallet rack uprights

Abstract. *This paper describes the experiments carried out at Oxford Brookes University to measure the local rotation of the upright at the connection of elements. The aim of this experimental investigation was to determine the reduction in stiffness due to distortion of the upright. The distortional stiffness was quantified and introduced into a three dimensional frame model by the use of an equivalent rotational spring with a further reduction of the discrepancy between the shear stiffness values determined by theory and experiment.*

1 INTRODUCTION

Pallet racks are regular beam and column structures. The columns are usually perforated cold-formed sections and the beams that lie in the plane of the aisles, also cold-formed, connect with the uprights using connectors with a semi-rigid moment-rotation characteristic. In cross-aisle planes the columns are normally part of a bolted lattice column structure.

In the plane of the aisles, sway buckling is the dominant mode of failure heavily influenced by the stiffness and strength of the beam to column connectors. In the plane normal to the aisle where the structure is triangulated, a linear analysis is normally sufficient for use in design. However, in some very tall racks, narrow frames may have a significant shear flexibility that could influence overall elastic buckling. The source of the shear flexibility is the softness of the open section, bolt looseness, the eccentricity of the bolted connections and the manner in which the bracing elements are attached [1] – [4]. The elastic buckling load of this lattice column assembly depends on its flexural stiffness and its shear stiffness; the shear stiffness is measured by test [5]. The US RMI code [6] is based upon Timoshenko [7] and the authors in references [1] – [3] have pointed out that the US code yields values of shear stiffness that are up to 20 times more than those obtained from test. The earlier research quantified the influence of joint eccentricity, bolt slip, bracing arrangement and recommended changes in test procedures so that all tests were conducted cyclically varying the load. The authors also recommended that cross-aisle looseness be included as ignoring this effect could cause significant errors in the prediction of the shear stiffness. However, the best theoretical models developed still only predicted stiffness values which were still approximately double those of the observed experimental ones. The objective of this paper was to investigate the influence of member distortion on the results.

2 EXPERIMENTAL INVESTIGATION

2.1 Test specimens

Tests were conducted on full sized upright frames made of cold formed steel sections conforming to EN 10147 [8]. The uprights were open perforated lipped channels with additional bends and the bracing members were lipped channels. The upright and bracing members used in testing are shown in Figure 1. Note that all

the dimensions mentioned are in mm. The cross- sectional properties of upright and bracing members that were used in the tests were: upright properties – area 788.9 mm^2, I_{yy} 522444 mm^4, I_{zz} 1.02x10^9 mm^4, the distance of the centroid of the upright from its back face centre line 33.96 mm and torsion constant 2062 mm^4; bracing member – area 139.5 mm^2, I_{yy} 27187 mm^4, I_{zz} 10923 mm^4, the distance of the centroid of the brace from its back face centre line 8.87 mm and the torsion constant 105 mm^4. The upright frames used in the distortion test had one panel of length (i.e. centre to centre distance between joints, where diagonals intersect) 1200mm and the depth of the frame was 1050mm leading to panel aspect ratio of 1.14.

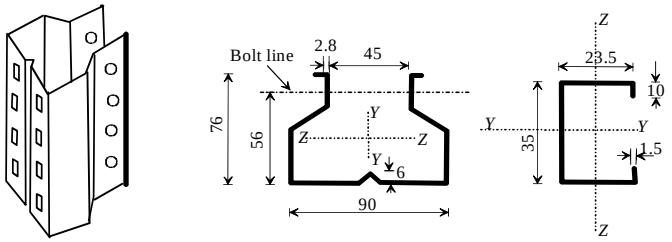

(a) A view of upright (b) Upright section (c) Brace section

Figure 1: Upright and bracing member dimensions.

2.2 Test arrangement

Earlier shear tests conducted on upright frames identified the significance of the lacing pattern (i.e. back-to-back or lip-to-lip) and the application of load on the frames [1] – [3]. Depending upon the orientation of the diagonal braces (called lacing elements) the forces in these elements can be in either tension or compression. It was assumed that the eccentric forces applied from lacing elements to the upright would lead to distortion of the upright, which in turn would reduce the shear stiffness. This experimental program was aimed at evaluating the accurate joint stiffness, which was then used further in numerical and theoretical analyses. In total, four tests were carried out by changing the lacing ('back-to-back' or 'lip-to-lip') and loading patterns (tension or compression in the loaded member). All the tests were conducted on single panel frames with restraints at the corner nodes of the frames only. The basic arrangement of the test upright frame and application of the load was similar to other tests by the authors [1] – [4]. However, more displacement transducers (LVDTs) were placed on the upright of the frame with connecting joint between lacing members and upright section as depicted in Figure 2. Test arrangements are shown in Figure 3. Figure 3(b) shows a 'lip-to-lip' lacing arrangement. Note that this arrangement would not normally be used in practice but was used in two of the tests to get different geometries. The 'back-to-back' pattern reduces eccentricities in the diagonal bracing.

Two LVDTs were used at locations A, C and D to measure the upright rotation under applied loading. 'A' and 'C' were located at midpoints of half panels and 'D' was 112.5 mm away from 'A'. At location B, as shown in Figure 2, two displacement transducers were placed in similar positions to those at A and also an extra two LVDTs were placed on the top of upright to measure difference in upright rotations at the joint, if any. The values measured during the experimental program were not at the exact locations where the LVDTs were placed since there was movement of the upright. They were approximately at ± 10 mm along the length of the upright. The data obtained from the data acquisition system was used to plot load-rotation curves as shown in Figures 4 and 5. Note that the initial loading curves from the origins have a different slope to those of subsequent cyclic curves. This is due to the initial looseness in the system. As these tests were solely to determine the effects of distortion this looseness was ignored and the regression lines obtained from the other data. Note that not conducting cyclic tests through zero is contrary to the authors' recommendations [4] but tests with both tensile and compressive loading were undertaken.

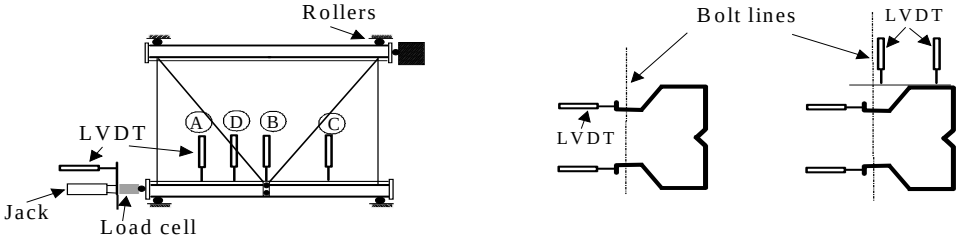

(a) Test Schematic (b) Detail at A, C and D (c) Detail at B

Figure 2: Test arrangement.

(a) Experimental set-up (b) Displacement transducer positions

Figure 3: Experimental arrangement.

2.3 Analysis of results

The cross-section of the uprights can distort in the modes shown in Figure 5. The original cross-section is shown in Figure 5(a).and the modes are: St. Venant torsion of the entire upright section [Figure 5(b)], the cross-section of the upright opening in a distortional mode [Figure 5(c)] and shear distortion of the cross-section [Figure 5(d)]. The mode shown in Figure 5(c) can either be inwards or outwards. This mode is approximately represented by a half-sine wave. In the test procedure this mode was suppressed at the central joint by the bolt attached to the bracing.

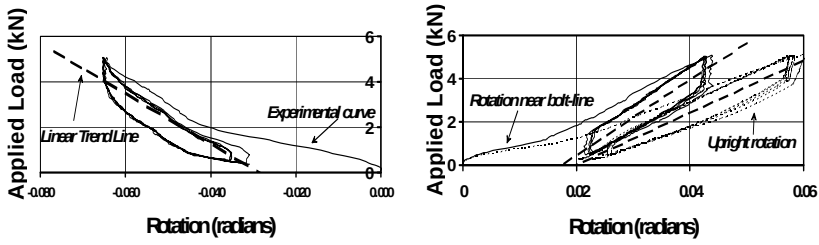

(a) Rotation at position A (b) Rotation at position B

Figure 4: Test results: Rotation at joints.

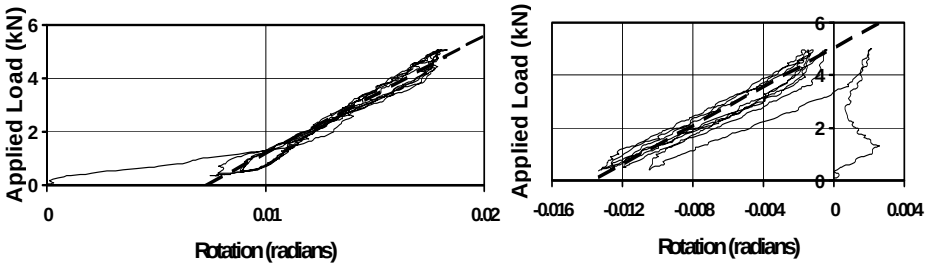

(c) Rotation at position C (d) Rotation at position D

Figure 4 (continued): Test results: Rotation at joints.

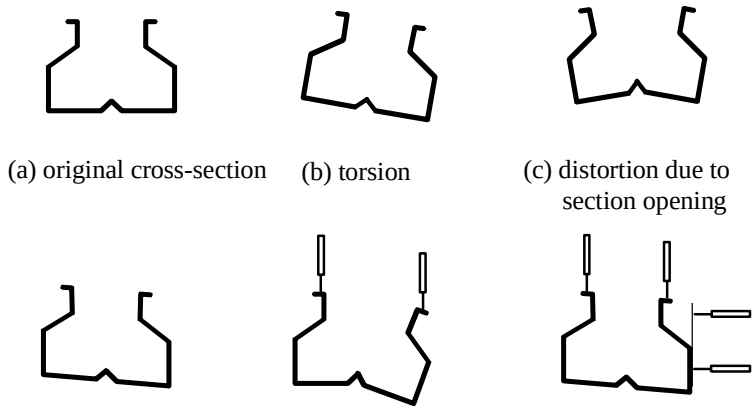

Figure 5: Upright distortion modes.

The positions of the transducers in relation to cross-sections is shown in Figures 5(e) [Positions A,C and D in the test] and 5(f) [Position B in the test]. Unfortunately, as can be seen in Figure 4 the transducer positions at A, C and D were not able to capture the distortion alone as they were affected by both types of distortion and by torsion. However the two pairs of transducers at B were successful. The transducers attached to the flange sides of the upright were only affected by torsion and hence the rotation that these transducers measured was only torsion. The transducers attached to the lips of the uprights were affected by both shear distortion and torsion. Hence removing the torsion effects gave estimates of change in angle due to distortion. Table 1 gives the results of the rotation measurements.

2.4 Calculation of rotational stiffness

The rotational calculations (θ) shown in Table 1 are measured in terms of load applied (P) on the upright frame. As we already know the geometry of the frame, we can calculate forces in the lacing members (F) by

simplifying the system as a truss. This simplistic assumption ignores the continuity of the upright at joint but is verified by the results of finite element analyses shown in Table 3 below where the difference in analyzing the frame as a pin-joined truss compared with analyzing it as a rigid frame is approximately 5%. The perpendicular component of these forces in lacing members generates distortion of the upright. Figure 6 gives a schematic of the frame.

Table 1: Rotation calculations

Load in upright	Lacing pattern	Vertical transducer (kN/rad)	Horizontal transducer (kN/rad)	Difference (kN/rad)	Mean (kN/rad)
Compression	Lip-to-lip	223.24	158.86	64.38	59.37
Tension	Lip-to-lip	173.31	119.96	53.35	
Compression	Back-to-back	432.37	324.53	107.84	103.20
Tension	Back-to-back	420.26	321.71	98.55	

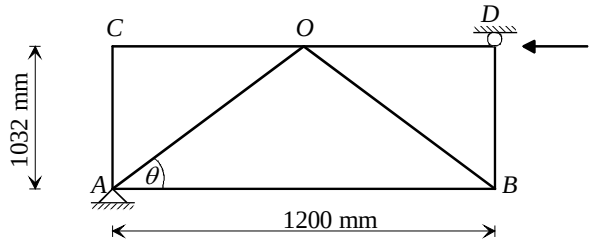

Figure 6: Loading schematic.

Assuming a load *P* is applied at point *D.* Resolving horizontally at the joint *O* the force in each bracing member is given by

$$\text{bracing member force} = \frac{P}{2\cos\theta} \tag{1}$$

For the tested frame

$$\cos(\theta) = \frac{600}{\sqrt{600^2 + 1032^2}} = 0.5026 \tag{2}$$

Hence force in each bracing member = *P**0.9958 kN.

The vertical components of the forces in the bracing elements generate a torque at the joint. The vertical component is

$$P\sin(q) = \frac{1032}{\sqrt{600^2 + 1032^2}} P = 0.8645P \tag{3}$$

The moment applied to the upright depends upon the bracing configuration as seen in Figure 7.

The distance of the centroid of the bracing from the back face was 8.87 mm. Hence as the bracing web was 25 mm from the front to the back the moment lever-arm of the eccentric forces was 2*(25.0-8.87) = 32.26 mm in the lip-to-lip case and was 2*8.87 = 17.74 mm in the back-to-back case.

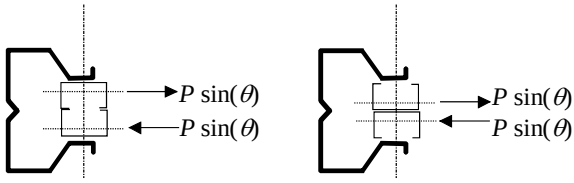

(a) lip-to-lip (b) back-to-back

Figure 7: Bracing forces.

The distortion rotational stiffness is given by

$$K = M/\theta = Fd/\theta = 0.8645*d*(P/\theta) \quad (4)$$

where M is the applied moment, θ the rotation, F is the bracing force and d the moment lever arm.

As the tests were conducted for tensile and compressive forces the mean value of (P/θ) is taken.

Hence:

Lip-to-lip Stiffness = 0.8645*32.26*59.37 = 1656 kN.mm/rad (5)

Back-to-back Stiffness = 0.8645*17.74*103.20 = 1583 kN.mm/rad (6)

Although the two rotational stiffnesses are almost the same this is thought to be a coincidence. In general they would be different.

3 NUMERICAL MODELING

A linear analysis was carried out on the frames using the LUSAS finite element software [9]. Initially a truss analysis was carried out using bar elements with translational degrees of freedom at each end. This produced results that were close to those of the RMI model but significantly higher than those produced by experiments. Hence the model was refined by using beam elements (4 elements per section, each element being derived from the Kirchoff theory [10] with translational and rotational degrees of freedom at each end and differential displacement at a mid-node. To account for the eccentricities caused by the centroidal distance of the upright from the line of action of the bolts connecting the bracing to the upright, bending in the bolt, eccentricity of the centroid of the bracing from the bolt axis small beam elements and spring elements were introduced to model the force transfer between bracing and upright. The spring elements had rotational and translational degrees of freedom. The joint model is shown in Figure 8. In the results below each different effect was added to the model in order to see the influence of each factor.

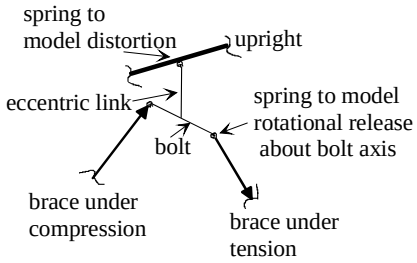

Figure 8: Forces at joint.

Table 3 shows a summary of the results obtained from the different analyses. In each case the stiffnesses obtained from tensile loads were averaged with those of compressive loads as in practical frames both tensile and compressive forces would act at different times upon the frame.

As the tests were only conducted on a single bay a sensitivity analysis was also undertaken where the distortional rotational stiffness was halved and doubled in value. The difference in results between the three cases was found to be negligible and hence is not included in Table 3.

The shear stiffness values from the tests are obtained by applying the equation

$$S = \frac{k_{ti} D^2}{L} \tag{7}$$

where S is the transverse shear stiffness, k_{ti} the slope of an experimental curve relating end displacement to applied load (see Figure 9), D the depth of the frame and L the total length of the frame [11].

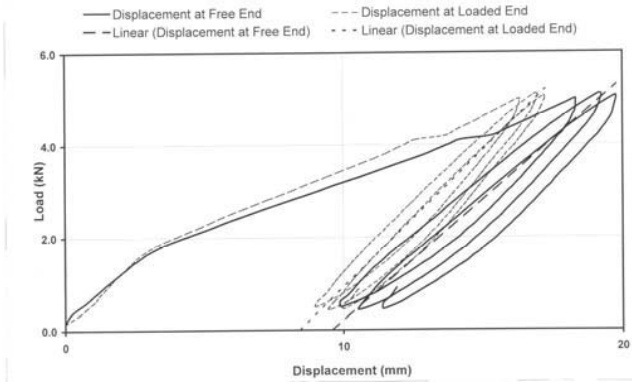

Figure 9: Experimental Shear stiffness determination.

Table 3: Numerical analysis results versus theoretical (RMI) and test values

FE model	RMI (kN)	Back-to-back braced frame		Lip-to-lip braced frame	
		LUSAS (kN)	Test (kN)	LUSAS (kN)	Test (kN)
Truss		8140		8140	
Rigid frame (A)		8675		8675	
Frame (A) with all eccentricities (B)		7502		6690	
Frame (B) + bolt bending (C)	10951	4372	1305	6688	643
Frame (C) + rotational release about bolt axis (D)		3003		3239	
Frame (D) + Affect of distortion		2756		1574	

Shear stiffness values obtained using rigid frame are higher than the results obtained using truss system due to the rigidity of the joints. As expected the affect of eccentricities were larger when lip-to-lip bracing pattern was used compared to a back-to-back bracing pattern. The bolt bending affect is more significant in the case of a back-to-back bracing patterned frame as the point of load transfer from the bracing members is at the centre of the bolt. As you also can see from Table 3, the rotation of bracing members on bolt axis

significantly reduces shear stiffness values. The affect of distortion is more pronounced in a lip-to-lip bracing patterned frame as the forces are applied more eccentrically. Though the inclusion of distortion reduces the difference between the numerical analysis results and the test values, still they differ by about two times. This could be due to initial looseness in the frame as reported by Beale et al [4] and the contact behaviour between various elements at the joints. This could be studied by more sophisticated three dimensional numerical models.

4 CONCLUSIONS

This paper describes the experiments carried out at Oxford Brookes University to measure the local rotation of the upright at the connection of elements. The distortional stiffness was quantified and introduced into a three dimensional frame model by the use of an equivalent rotational spring with a further reduction of the discrepancy between the shear stiffness values determined by theory and experiment. Though the inclusion of distortion reduces the difference between numerical analysis results and the test values, still they differ by about two times. This could be due to initial looseness in the frame and the contact behaviour between various elements at the joints, which could be studied by three dimensional numerical models.

REFERENCES

[1] Sambasiva Rao, S., Beale, R.G. and Godley, M.H.R., "Shear Stiffness of Pallet Rack Upright Frames", *Proc. 17th Int. Speciality Conf. on Cold-Formed Steel Structures*, Orlando, 295-311, 2004.

[2] Sajja, SR, Beale, R.G. and Godley, M.H.R., "Factors affecting the shear stiffness of pallet rack uprights", *Proc. Int. Colloquium on Stability and Ductility of Steel Structures*, Lisbon, 365-372, 2006.

[3] Sajja, S.R., Beale, R.G. and Godley, M.H.R., "Shear Stiffness of pallet rack upright frames", *Journal of Constructional Steel Research*, 64, 867-874, 2008.

[4] Godley, M.H.R. and Beale, R.G., "Investigation of the effects of looseness of bracing components in the cross-aisle direction on the ultimate load-carrying capacity of pallet rack frames", *Thin-walled Structures*, 46, 848-854, 2008.

[5] BSI, BS EN15512, "Steel static storage systems – Adjustable pallet racking systems – principles for structural design", *British Standards Institution*, London, 2009.

[6] The Rack Manufacturers' Institute, *Specification for the design, testing and utilization of industrial steel storage racks*, 1997.

[7] Timoshenko S. and Gere J., *Theory of Elastic Stability*, McGraw-Hill, US, 1961.

[8] BSI, BS EN10147, "Continuously hot-dip zinc coated structural steels strip and sheet. Technical delivery conditions", *British Standards Institution*, London, 2000.

[9] FEA Ltd, *LUSAS 13.8 user manual*, London, UK, 2006.

[10] FEA Ltd, *Lusas Theory Manual*, London, UK, 2000.

[11] British Standards Institute, *BS EN 15512:2009, Steel Static Storage Systems – Adjustable pallet racking systems – Principles for structural design*, London, UK, 2009.

SDSS'Rio 2010 STABILITY AND DUCTILITY OF STEEL STRUCTURES
E. Batista, P. Vellasco, L. de Lima (Eds.)
Rio de Janeiro, Brazil, September 8 - 10, 2010

BUCKLING, POST-BUCKLING, COLLAPSE AND DESIGN OF TWO-SPAN COLD-FORMED STEEL BEAMS

Cilmar Basaglia and Dinar Camotim

Department of Civil Engineering and Architecture, ICIST/IST, Technical University of Lisbon, Portugal
e-mails: cbasaglia@civil.ist.utl.pt, dcamotim@civil.ist.utl.pt

Keywords: Cold-formed steel, Two-span continuous beam, Buckling, Post-buckling, Structural design

Abstract. *This paper reports the available results of an ongoing numerical investigation on the buckling, post-buckling, collapse and design of two-span cold-formed steel lipped channel beams subjected to uniformly distributed loads. The results presented and discussed are obtained through analyses based on Generalised Beam Theory (elastic buckling analyses) and shell finite element models (elastic and elastic-plastic post-buckling analyses up to collapse). Moreover, the ultimate loads obtained are used to establish preliminary guidelines concerning the design of continuous (multi-span) cold-formed steel beams failing in modes that combine local, distortional and global features. An approach based on the existing Direct Strength Method (DSM) expressions is followed and the comparison between the numerical and predicted ultimate loads makes it possible to draw some conclusions concerning the issues that must be addressed by a DSM design procedure for cold-formed continuous beams.*

1 INTRODUCTION

In order to adequately design and assess the structural efficiency of cold-formed steel (thin-walled) members one must acquire in-depth knowledge on their non-linear response, a complex task that requires evaluating buckling stresses and determining post-buckling equilibrium paths up to collapse (accounting for initial imperfections). Indeed, a fair amount of research work has been recently devoted to the development of efficient design rules for isolated thin-walled members. The most successful end product of this research activity was the increasingly popular "Direct Strength Method" (DSM) [1], already included in the current Australian/New Zealander (AS/NZS4600: 2005) and North American (NAS: AISI-S100-07) specifications for cold-formed steel structures.

In practice, many thin-walled structural members exhibit multiple spans (*e.g.*, secondary elements like purlins or side rails) and are often subjected to non-uniform bending moment diagrams that combine positive (sagging) and negative (hogging) regions, a feature making their buckling behaviour rather complex, as it often (i) combines local, distortional and global features and (ii) involves a fair amount of localisation (*e.g.*, the occurrence of local and/or distortional buckling in the vicinity of the intermediate supports, where there are significant moment gradients and very little restraint can be offered to the slender bottom/compressed flanges). Even so, it seems fair to say that it is still very scarce the amount of research on the buckling and post-buckling behaviours of thin-walled steel beams subjected to non-uniform bending moment diagrams, namely continuous beams. In this context, it is worth mentioning the recent works of (i) Camotim *et al.* [2], who used Generalised Beam Theory (GBT) to analyse the buckling behaviour of steel beams with distinct loadings and support conditions (including intermediate supports), and (ii) Yu and Schafer [3], who investigated the influence of a linear bending moment gradient on the distortional buckling and post-buckling behaviours of single-span cold-formed steel beams, and used their finding to examine and extend the DSM design procedure for such members.

The aim of this work is to present and discuss the results of an ongoing numerical investigation on the buckling, post-buckling, collapse and DSM design of two-span lipped channel beams. The numerical results presented were obtained through (i) GBT buckling analyses and (ii) elastic and elastic-plastic shell finite element (SFE) post-buckling analyses. In particular, some interesting conclusions are drawn on the features that must be incorporated in a DSM design procedure for this type of cold-formed steel members.